Nanodiamond-Based PP/EPDM Thermoplastic Elastomer Composites: Microstructure, Tribo-Dynamic, and Thermal Properties

F. Hejazi Jahromi, A. A. Katbab

Department of Polymer Engineering and Color Technology, Amirkabir University of Technology, Tehran, Iran

Received 5 March 2011; accepted 6 October 2011
DOI 10.1002/app.36299
Published online 18 January 2012 in Wiley Online Library (wileyonlinelibrary.com).

ABSTRACT: Attempts have been made for the first time to employ graphitized nanodiamond with the cage-like structure to prepare thermoplastic elastomer (TPE) nanocomposites based on polypropylene (PP) and ethylene-propylene-diene rubber (EPDM), with improved tribo-dynamic properties. Samples were prepared via melt mixing process, and maleated polypropylene (PP-*g*-MAH) was used to promote the interfacial interactions between the components and partitioning of nanodiamond particles in polymer phases. Microstructure characterization revealed significant reduction in the size of EPDM droplets if nanodiamond particles are preferentially wetted by the polypropylene phase. Nanoindentation and scratch tests performed on the surface of prepared nanocomposites exhibited enhanced surface stiffness and scratch resistance. Rheomechanical spectroscopy (RMS) and dynamic mechanical analysis (DMTA) showed enhanced melt elasticity for the interfacially compatibilized nanocomposites, which is attributed to the antiplasticizing characteristics of the caged shape nanodiamond particles. More interestingly, nanodiamond particles exhibited plasticizing behavior for the nanocomposite in molten state. All interfacially compatibilized nanodiamond composites showed enhanced thermal resistivity. © 2012 Wiley Periodicals, Inc. J Appl Polym Sci 125: 1942–1950, 2012

Key words: thermoplastic elastomer (TPE); nanodiamond; tribological properties; PP/EPDM

INTRODUCTION

Thermoplastic elastomer (TPE) blends based on polypropylene (PP) and EPDM rubber have been used in a wide range of applications such as automotive industry, where enhanced mechanical properties, thermal stability, scratch, and wear resistance are essential. In TPE materials, the thermoplastic phase forms the main matrix, and the elastomer is dispersed in the form of aggregated droplets. The dispersed elastomer phase serves to improve and control the toughness and low-temperature impact resistance. Nanofillers are commonly incorporated into TPE's formulation to increase stiffness, dimensional stability, and modify properties.

Molecular diamond (called nanodiamond) is thermodynamically stable molecule found in natural gas/petroleum streams,[1–4] and composed of all trans-fused cyclohexane rings. The initial diamondoid series of hydrocarbons possess the chemical formula C4*n*+6 H4*n*+12, where *n* indicates the number of diamond-cage subunits, which is isostructural with macroscopic diamonds. These hydrocarbons can be considered to form a continuous structural series including lower diamondoids (molecular diameter <1 nm), higher diamonds (_1–2 nm), nanocrystalline and chemical-vapor-deposition diamonds (with the size of 2 nm to few micrometers), and macroscopic diamonds.[5–7]

The smallest member of this family, adamantane (C10H16), has a single cage-shaped subunit excised from the diamond crystal lattice with dangling carbon bonds terminated with hydrogen atoms. Each successive member of the diamond family contains one additional face-fused diamond crystal lattice cage. Diamantane and triamantane contain two and three fused face cages respectively. Tetramantane has four isomers that result from fusing of four cages. The diamond face-fused cage structure of these materials leads to their stability, strength, and rigidity.[8]

Nanoscale diamond is a valuable additive to be used in multifunctional polymer composites especially for the purposes where a combination of mechanical, thermal, tribological, and dielectric properties is expected.[9–12]

Polymer nanocomposites have attracted extensive research interests in recent years. It has been found that these materials have many advantages over traditional polymer composites with microscale fillers such as increased strength (without degrading other mechanical properties), decreased gas permeability,

Correspondence to: A. A. Katbab (Katbab@aut.ac.ir).

improved heat resistance, and enhanced electrical conductivity.[13] In comparison with inorganic fillers such as silica, clays, and ZnO, organic nanodiamond is potentially more easily dispersed in organic polymer materials.[14] This work addresses the peculiarities of ultra dispersed graphitized nanodiamond powder when incorporated into the structure of PP/EPDM thermoplastic elastomer (TPE), and its impact upon the micromorphology, thermal, mechanical, and Tribological behavior of corresponding nanocomposite TPE have been studied.

EXPERIMENTAL

Materials

The polypropylene used in this work was isotactic and injection grade with commercial name of EP2X 83CI (Arak, Iran). The EPDM rubber with trade name of KEP 330 having 7.9 wt % ENB as diene monomer and mooney viscosity of ML(1-4)100°C = 24 produced by KELTAN Company (Korea) was used as the dispersed rubber phase. Maleic anhydride grafted polypropylene with melt flow index (MFI) of 40 $\frac{gr}{10\ min}$ and maleation percent of 0.5–0.8 manufactured by Pluss Polymer Company (India) with the commercial name of OPTIM P406 was employed as compatibilizer. Ultra dispersed graphitized diamond (average particle size of 3–6 nm) supplied by ALIT (Ukraine) was employed as nanofiller.

Composites preparation

Polypropylene and EPDM with the ratio of 70 to 30 (w/w %) respectively, were melt blended with different percentage of nanodiamond (3 and 5 wt %) in a Brabender Plasticator PL 2200 model internal mixer. Blending process was carried out at 175°C and mixing speed of 60 and 120 rpm for 10 min. Samples were then injection molded into proper shapes for mechanical testing using an ES 15060 model Injection machine (Australia). Thin sheets with the thickness of 3 mm were also prepared via compression molding method by means of a hydraulic press at 200°C.

Characterization

Wide-angle X-ray diffraction

Wide-angle X-ray diffraction (WXRD) measurements were conducted on sample surface at room temperature (23°C) using a XPERT X-ray diffractometer in the normal reflection mode with Ni-filtered Cu Kα radiation (λ = 1.54 Å) and a step size of 0.02°C (2Θ) and a holding time of 1 s.

Scanning electron microscopy

The micromorphology of PP/EPDM/diamond nanocomposites was studied by use of scanning electron Microscope model XL30 made be philips (Eindhoven, The Netherlands). For this purpose, cryofractured surfaces of samples were gold coated, by sputtering technique.

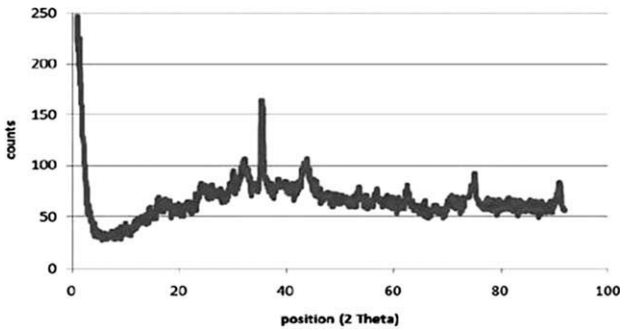

Figure 1 WXRD profile of the used nanodiamond powder.

Melt viscoelastic behavior

Linear melt viscoelastic characteristics of the prepared nanocomposites were measured at 190°C using a Paar Physica USD 200 melt rheometer. The dynamic shear measurements were performed in osillation mode and parallel-plate geometry with the plate diameter of 2.5 mm and the plate gap setting of ~1 mm, by applying time dependent strain. The frequency ranges were varied between 0.1 and 630 rad/s and the strain amplitude was applied to be within the linear viscoelastic ranges.

Dynamic mechanical analysis

A TriTec 200 DMA model DMA-TRITON was used with bending mode at an oscillatory frequency of 1 Hz and an applied strain of 0.5% at a heating rate of 10°C/min for all samples. The temperature scan was performed from –60 to 170°C. The samples were tested in the form of disk with the dimensions of 10 mm length, 5 mm width, and 1–1.3 mm thickness.

Nanoindentation and nanoscratching measurements

To examine the extent of improvement in indentation and surface scratch resistance of the prepared samples, a Hysitron. TriboScope Nanomechanical Test Instrument with a two-dimensional transducer, leveling device and complete software in combination with a blunt ($R^1/_4$200 nm) three-sided diamond indenter was used. The indented surface was firmly mounted on an AFM stage of a nanoscope III instrument for direct measurement of the initial surface (suitability and slope correction) and of the final impression, using the same indenter tip (though with some tip sample convolution). The Triboscope recording unit with transducers and leveling device was placed on top of the NanoScope III E

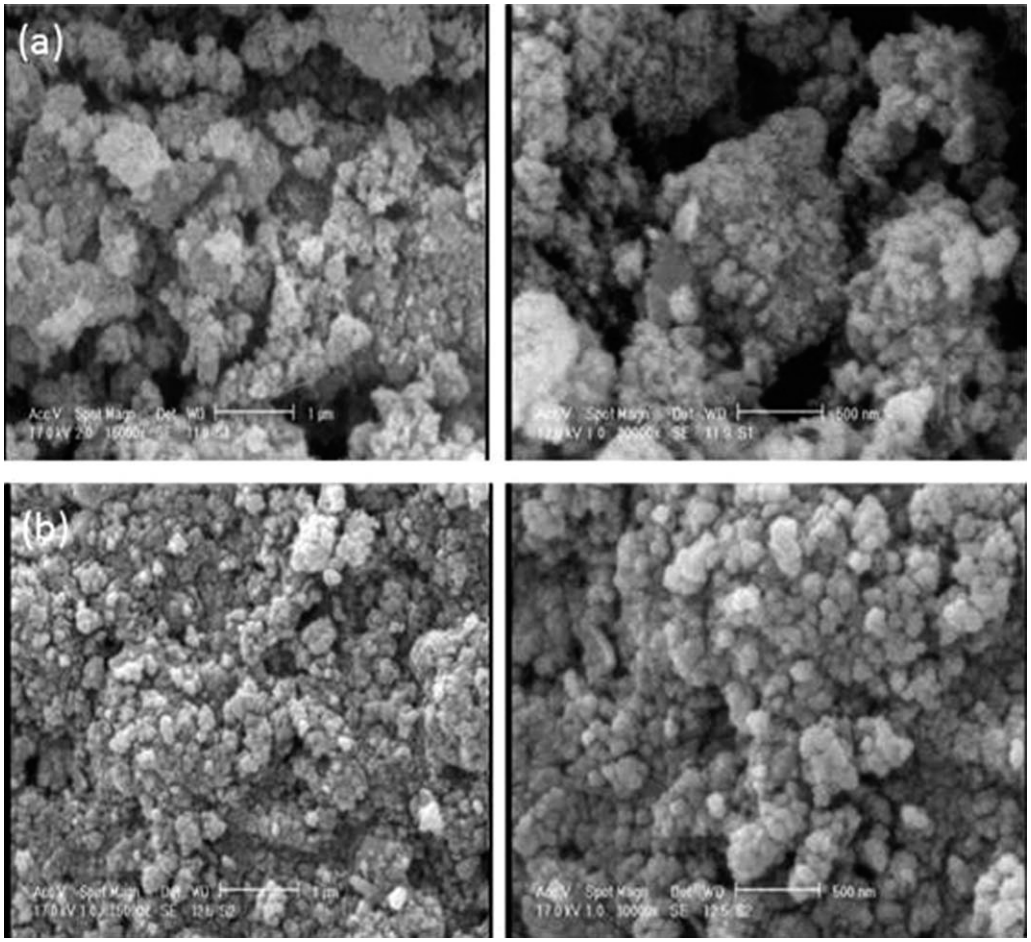

Figure 2 SEM images of: (a) pristine nanodiamond powder, (b) nanodiamond powder after sonication process for 5 min.

164 _ 164 mm2 XY piezo scan base for that purpose. More detailed AFM images were obtained with Si3N4 cantilever tips.[15] Load and unload times were 30 s, holding times 10 s at the indentations. Constant force edge-in-front nanoscratchings of 4 mm length were performed in 30 s at constant rate after the initial indentation. The F_L, effective F_N and depth values were averaged with Excel software from the central 33% of the scratching traces that were recorded.

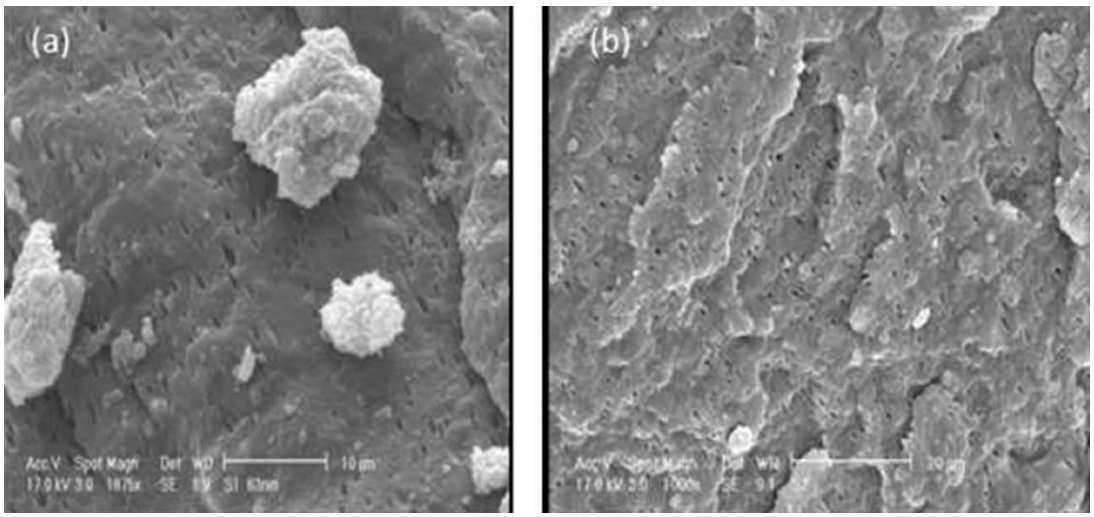

Figure 3 SEM images of nanocomposites composed of 5% nanodiamond prepared at mixing rates of: (a) 60 rpm, (b) 120 rpm.

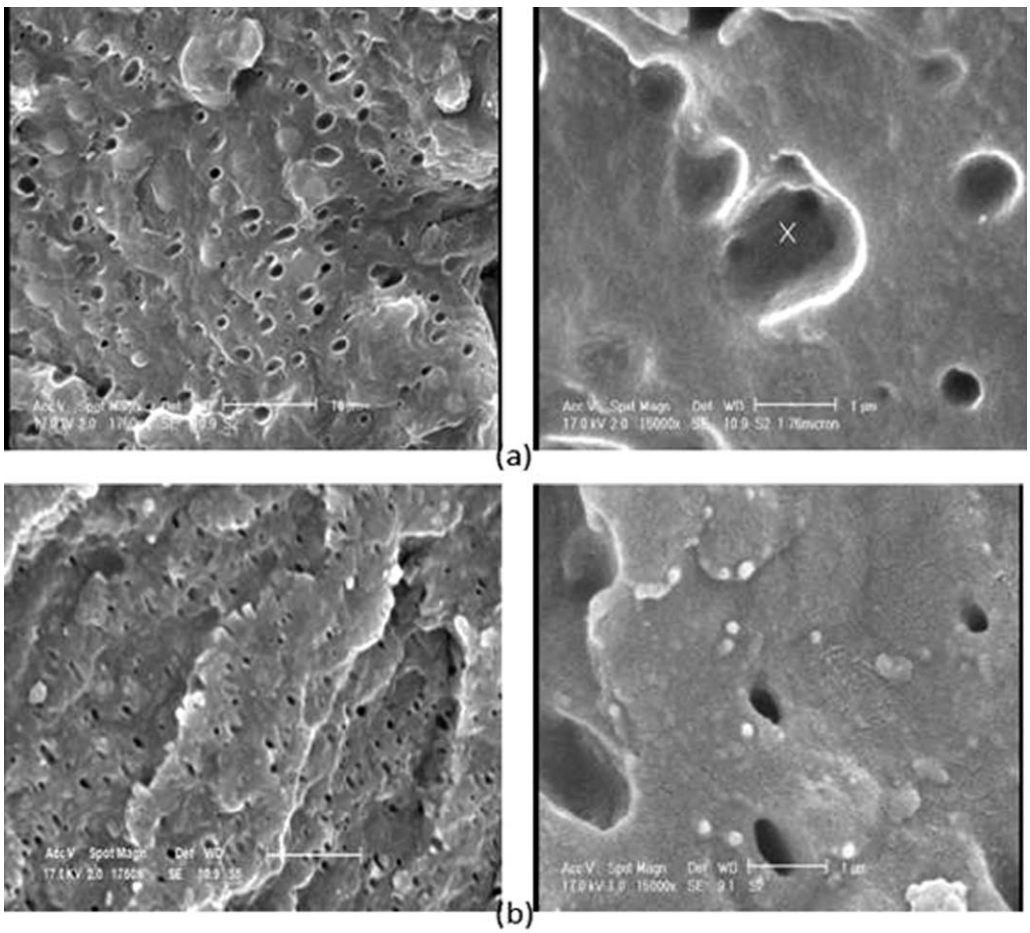

Figure 4 SEM images of composites composed of: (a) PP/EPDM+5% PP-*g*-MAH (120 rpm), (b) PP/EPDM+5% PP-*g*-MAH+5% ND (120 rpm).

Thermal stability evaluation of nanocomposites

The thermal stability of the composites was analyzed by thermogravimetric analysis (TGA) with a PLTGA model Thermo Gravimetric Analyzer. The sample sizes ranged from 9 to 13 mg. The samples were heated at heating rate of about 10°C/min from 20 to 600°C under a dry nitrogen purge of 50 mL/min.

RESULTS AND DISCUSSION

Crystallinity of the nanodiamond

Figure 1 shows the WXRD patterns of the used nanodiamond. The presence of three broad peaks at $2\theta = 43.8°$, 75.2°, and 91.1° corresponding to the (111), (220), and (311) diamond planes, demonstrates

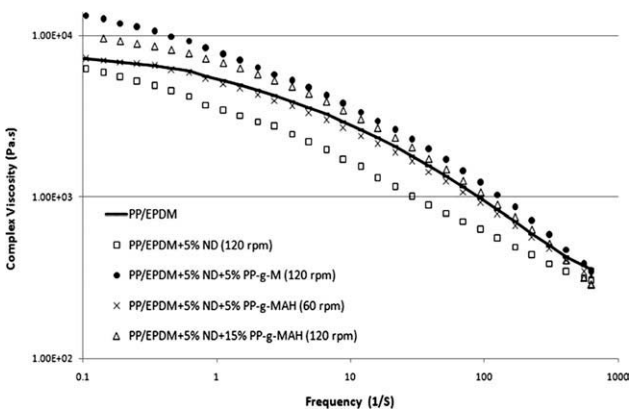

Figure 5 Variation of melt viscosity versus frequency for various prepared PP/EPDM/nanodiamond composites.

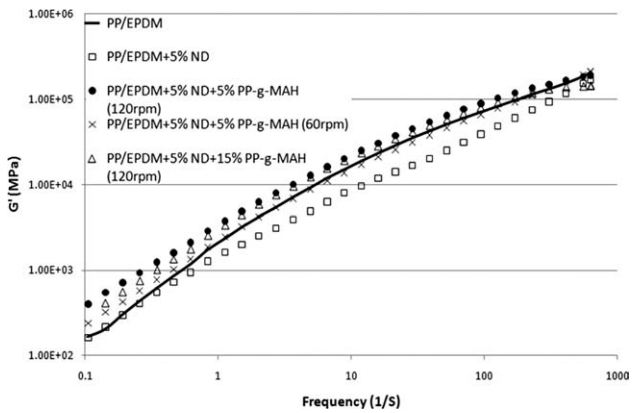

Figure 6 Dynamic storage modulus versus frequency for various prepared PP/EPDM/nanodiamond composites.

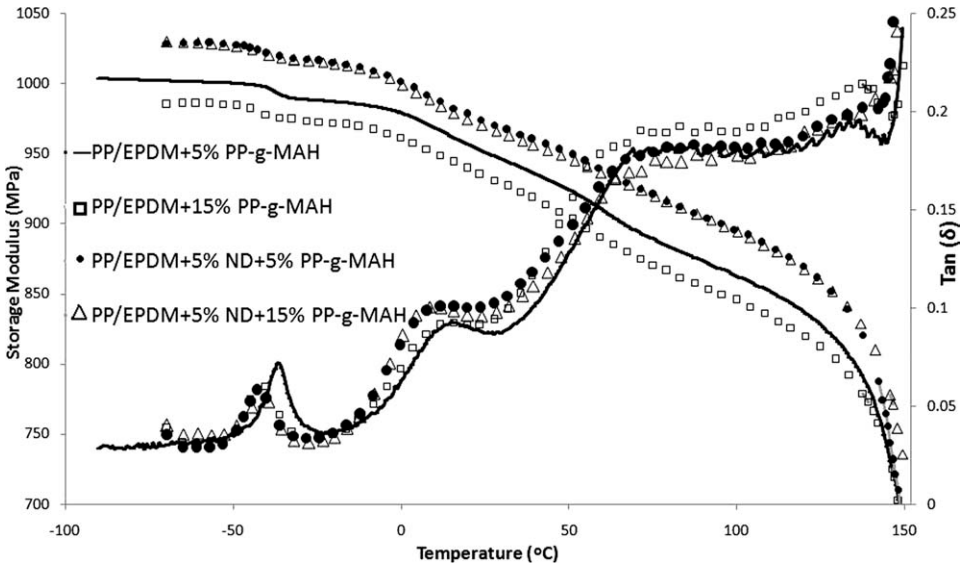

Figure 7 Storage modulud and loss tangent as a function of temprature for various prepared PP/EPDM/nanodiamond composites.

that the geometry of nanodiamond crystal is in the form of cubic.[16] The diamond (111) planes are composed of zigzag hexagonal rings that can be easily rearranged into graphite sheets. Therefore, the graphite fragments with different numbers of carbon atoms exfoliate from the external surface of any diamond (111) plane and surround diamond particles. These fragments are rearranged by introducing pentagonal and other polygonal rings to form a closed shell. As a result of this process, diffraction peaks of diamond weaken and graphite peaks also appear in the XRD pattern of the selected nanodiamond.[17] Therefore, the peak at $2\theta = 24.9^\circ$ corresponds to (002) graphite planes. On this basis, in addition to (111) diamond planes, a fraction of the intensity of the peak at $2\theta = 43.8^\circ$ is related to the graphite (100) planes. XRD patterns of adamantane, diamantane and triamantane exhibit three diffraction peaks at diffraction angles of $2\theta = 35.4^\circ$, 32 and 16°.[14,18,19] Accordingly, the nanodiamond powder used in this work was mainly composed of adamantane and partly diamantane and triamantane.

Morphological studies

The scanning electron microscopy (SEM) images of pristine ND and the ND which was sonicated for 5 min in *N*-methylpyrrolidone (NMP) are shown in Figure 2(a,b). The pristine ND exhibits highly agglomerate feature which is attributed to the high interactions between nanosize particles. It is obvious that sonication technique can break these clusters to smaller sizes. The average diameter of each cluster before and after sonication was measured to be 1000 and 200 nm, respectively. Although sonication technique could improve the dispersion of nano particles in polymer matrix, but, pristine ND was employed to make nanocomposite (as sonication is a time consuming process). Effect of the mixing speed on dispersion of nanodiamond is shown in Figure 3. The morphologies of the prepared TPE composites and ND/TPE nanocomposite are also presented in Figure 4. It can be seen that the presence of ND particles in TPE matrix significantly has reduced the size of EPDM droplets in PP continues phase. The voids appeared in SEM micrographs are related to the EPDM droplets on the cryofractured surface.

TABLE I
Dynamic Storage Modulus at 25°C and Teransition Tempratures for Various Prepared PP/EPDM/Nanodiamond Composites

Sample	Storage modulus (*E*), (MPa)	Transition temperature (°C)	Transition temperature (°C)	Transition temperature (°C)
PP/EPDM+5% ND+5% PP-*g*-MAH	972.65	−42	11.4	–
PP/EPDM+5% PP-*g*-MAH	951	−36.18	15.74	135.8
PP/EPDM+5% ND+15% PP-*g*-MAH	969.72	−41.5	10.78	–
PP/EPDM+15% PP-*g*-MAH	933.52	−42	15.74	136.5

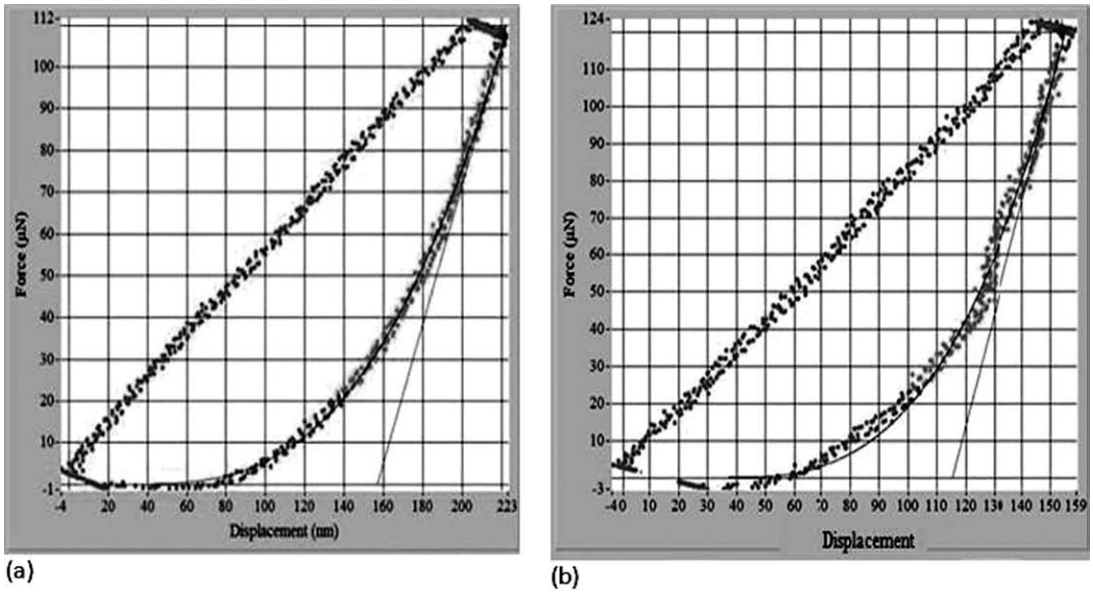

Figure 8 Analysis of the indentation unloading curves of (a) PP/EPDM+5% PP-*g*-MAH, (b) PP/EPDM +5% ND +5% PP-*g*-MAH.

Reduction in the size of the dispersed rubber phase is expected to improve the impact resistance of the corresponding nanocomposite.

Rheological behavior and dynamic mechanical analysis

Figures 5 and 6 illustrate the plots of melt complex viscosity and dynamic storage modulus versus frequency for the unfilled PP/EPDM simple blend (70/30, w:w) and corresponding nanocomposites respectively. It is clearly observed that incorporation of 5 wt % of nanodiamond in the absence of PP-*g*-MAH, has led to the decrease in both melt viscosity and storage modulus, which implies the lubricating behavior of nanodiamond particles for the polymer matrix. However, the interfacially compatibilized TPE/nanodiamond composites exhibited higher viscosity as well as melt elasticity within both low and high frequency regimes. These evidenced the reinforcement of interfaces between nanodiamond particles and PP/EPDM matrix. Moreover, increasing the PP-*g*-MAH to nanodiamond ratio from 1 : 1 to 3 : 1 did not show significant effect upon melt dynamic behavior of the prepared nanocomposites. However, the extent of enhancement is not significant compared to other reinforcing nanofillers such as nanoclay and carbon nanotube (CNT), which is attributed to the lubricating characteristics of nanodiamond in molten polymer matrixes.

These results are consistent with dynamic mechanical behavior of the prepared PP/EPDM/nanodiamond

TABLE II
Nanoindentation Analysis of the Prepared Samples

Characteristics	PP/EPDM +5% PP-*g*-MAH	PP/EPDM+5% PP-*g*-MAH+ 5% ND	Increase or decrease in characteristics
Reduced modulus	1.2	2.9	142% increase
Hardness (GPa)	0.07	0.14	100% increase
Stiffness (μN/nm)	1.7	3	76% increase
Contact depth (nm)	173.2	125.5	30% decrease
Max depth (nm)	223.2	158.9	30% decrease
Max force (μN)	107/8	120.8	12% increase
Contact area	1.523	8.567	44% decrease
Total indentation work (J) (for 150 nm displacement)	6	9	50% increase
Elastic work (J) (for 150 nm displacement)	0.8	3.07	162% increase in the fraction of elastic work
Plastic work (J) (for 150 nm displacement)	5.2	5.93	25% decrease in the fraction of plastic work

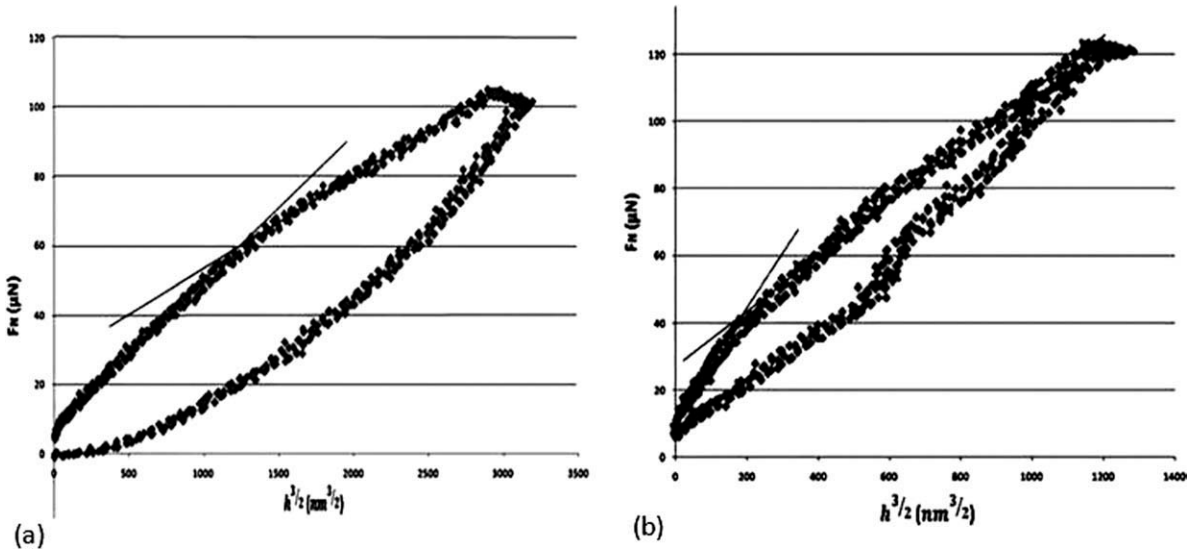

Figure 9 Analysis of the indentation loading curves of (a) PP/EPDM+5% PP-*g*-MAH, (b) PP/EPDM +5% ND +5% PP-*g*-MAH.

composites as illustrated in Figure 7 and Table I. Inclusion of nanodiamond particles onto the PP/EPDM blend system led to the displacement of EPDM and PP thermal transition peaks to higher temperatures. Enhanced bending modulus exhibited by nanocomposites generated by the incorporation of 5 wt% nanodiamond is explained to be attributed to the antiplasticization behavior of nanodiamond for the polymer matrix in solid state. Antiplasticization can be defined as a simultaneous decrease in T_g with increased mechanical stiffening and embrittlement caused by the incorporation of particulate nanofiller has been explained to be due to the reduction of the free volume of the polymer matrix and consequently restriction of local, noncooperative in-chain molecular motions. The most important characteristics of an antiplasticizer is that it behaves similar to the common plasticizers in the molten state but as reinforcing fillers below the polymer glass transition temperature (T_g).[14] The observed antiplastisizing effect by nanodiamond is related to the cage-like structure of nanodiamond particles which enables the polymer segments to be interlocked. The observed reduction of glass transition is due to the increase in the free volume between nonrestricted chains that results in the mobility of these chains in lower temperatures. Moreover, incorporation of nanodiamond particles caused removal of the PP α-transition which needs to be more investigated in the future research works.

Nanoindentation measurement

The surface stiffness and resistance to indentation of an indenter were evaluated by conducting nanoindentation test, and variation of the applied force versus displacement of the indenter in the sample was analyzed. Figure 8 illustrates the loading-unloading curves of the indentation test performed on the unfilled PP/EPDM blend sample and its corresponding nanocomposites. After required calibrations[20] and fittings according to the Olive and Pharr method,[20] the resultant parameters are summarized in Table II.

On the basis of the results presented in Figure 8 and Table II, the sample containing nanodiamond exhibited significant increase in reduced modulus, hardness and stiffness by 142, 100, and 76%, respectively. The surface resistance to indentation is defined as the required work to apply a definite displacement of the indenter in the sample (area under the loading curve). It is obvious that surface indentation resistance of diamond based nanocomposite is much higher than unfilled PP/EPDM blend. The area under the unloading curve accounts for the elastic work, and the area between loading and unloading curves represent the plastic work. It is clearly seen that the incorporation of 5 wt % nanodiamond into the PP/EPDM blend, led to the enhanced elasticity and tendency to recover the applied deformation. These observations lead to the conclusion that conformational changes by the applied deformation for the polymeric chains in contact with the nanodiamond particles

TABLE III
Nanoindentation Coefficients and Kink Positions of the Samples

Sample	k_1 ($\mu N/nm^{\frac{3}{2}}$)	k_2 ($\mu N/nm^{\frac{3}{2}}$)	Kink position (h, F_N)
PP/EPDM+5% PP-*g*-MAH	0.0417	0.026	(120.14, 61.6)
PP/EPDM+5% PP-*g*-MAH+5% ND	0.1387	0.0831	(35.58, 41.76)

TABLE IV
Nanoscratching Parameters of the Prepared Samples

Sample code	F_L (μN)	F_N (μN)	Scratch coefficient ($\mu N^{\frac{-1}{2}}$)	Specific nanoscratching work ($\mu N \cdot \mu m$)	Full scratch resistance (N/m)
PP/EPDM+5% PP-*g*-MAH	34.81	101.6	0.0342	34.81	10.87*1000
PP/EPDM+5% PP-*g*-MAH+5% ND	40.32	106.975	0.0364	40.32	12.6*1000

would not be thermodynamically favorable, and hence tendency for recovery of the original conformations is enhanced when the load is removed from the surface.

In addition to these parameters that can be achieved by analyzing the unloading curves, quantitative analysis of the loading curves in $F_N - h^{\frac{3}{2}}$ plots (Fig. 9), provides nanoindentation coefficients k (mN $nm^{\frac{-3}{2}}$) as the slopes of linear plots that reliably characterize the pristine polymers and are potent interpolation tools. Kinks in these linear plots (Fig. 9) indicate plastic-viscoelastic transformations and separate the characterization of the degraded polymer with the smaller nanoindentation coefficients from the pristine polymer.[15] The kink in unfilled PP/EPDM sample is attributed to the change in crystalline structure. However, for the PP/EPDM/nanodiamond composite, the kink could be attributed to the breaking of the nanodiamond physical structures in addition to the change in crystalline structures. So, in nanocomposite this kink occurred in lower displacement compared to the unfilled PP/EPDM blend. Sample's nanoindentation coefficients are summarized in Table III. As it can be seen in this table, incorporation of nanodiamond enhanced this coefficient.

Nanoscratching behavior

Nanoscratching test performed on the PP/EPDM simple blend sample and corresponding nanodiamond composite. According to the results, introducing a same scratch to the composite containing nanodiamond needs higher force (Table IV) and with an equal force, a smaller scratch can be applied on the nanocomposite compare to without-nano composite. Only the quantitative treatment with K from eq. (1) is an extrapolation tool that characterizes the mechanics upon nanoscratching (e.g., nonlinearity between normal force and lateral force; scratch work; scratch resistance). The nanoscratching work is lateral force times scratch length; the specific nanoscratching work spec Wsc (mN mm) is a characteristic parameter. It is equal to F_L times 1 mm according to eq. (2). The full scratch resistance (Rsc)tot is the scratch work divided by the cross-section of the scratch, which can be calculated from the recorded depth and the geometry of the indenter tip leading to proportionalities of (Rsc)tot and $F_L^{\frac{1}{3}}$ or $F_N^{\frac{1}{2}}$ (equation (3))[15].

$$K = F_L \Big/ F_N^{\frac{1}{2}} \tag{1}$$

$$\text{Spec } W_{sc} = F_L * 1 = K * F_N^{\frac{1}{2}} \tag{2}$$

$$(R_{sc})_{tot} = \frac{\text{Spec } W_{sc}}{A}, \tag{3}$$

where A is the cross section of the scratch.

The resultant parameters are summarized in Table IV. These parameters indicate the improved scratch resistance of thermoplastic elastomer by 16% with the incorporation of 5% nanodiamond.

Thermal stability of the composites

Thermal stability of polymer composites is one of the most important factors for polymer processing and aimed industrial application of polymers. The TGA thermograms of the various diamond nanocomposites are compared with unfilled counterpart samples in Figure 10 and Table V. As can be seen, thermal decomposition temperatures and the residual yields of PP/EPDM/nanodiamond composites increased compare to the PP/EPDM simple blend. Also, these factors increased with increasing ND level, implying that thermal decomposition of the

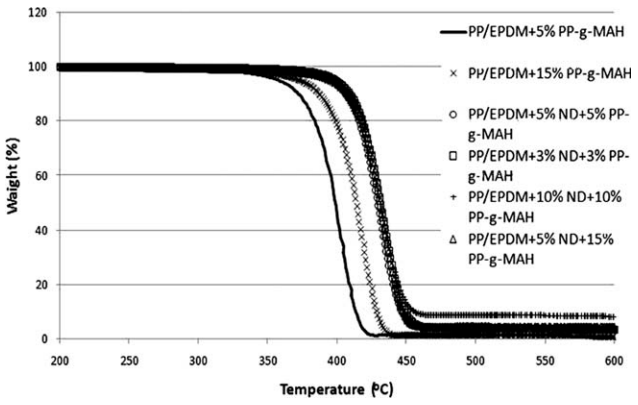

Figure 10 Thermal gravimetric analysis (TGA) of PP/EPDM/nanodiamond composite samples.

TABLE V
Thermal Gravimetric Analysis Results

Sample	Thermal decomposition temperature (°C)	Residual yield (%)
PP/EPDM+5%PP-*g*-MAH	343.53	0.37
PP/EPDM +15%PP-*g*-MAH	358.73	0.40
PP/EPDM+3%ND+3%PP-*g*-MAH	383.99	3.2
PP/EPDM+5%ND+5%PP-*g*-MAH	388.61	4.68
PP/EPDM+10%ND+10%PP-*g*-MAH	388.71	8.6
PP/EPDM+5% ND+15%PP-*g*-MAH	389	4.7

TPE/ND composites is retarded by incorporating ND into the TPE matrix with higher residual yield. This can be explained to be due to the thermal shielding behavior of nanodiamond in the polymer matrixes. In another word, nanodiamond, with high thermal stability, bears a large portion of the thermal energy, leading to the increase of the decomposition temperature of sample.

CONCLUSIONS

Incorporation of nanodiamond powder into thermoplastic elastomers showed significant effects on the morphology of blend system. Good dispersion of nanodiamond particles was achieved by increasing the mixing speed in internal mixer. The used nanodiamond acts as antiplasticizing nanoscale filler in PP/EPDM TPE system. These composites exhibited increased dynamic storage modulus, and reduced glass transition. Rheological behavior of the prepared TPE nanocomposites showed lubrication effect by the nanodiamond particles in the absence of PP-*g*-MAH, but, enhancement in melt viscosity and storage modulus when compatibilizer was incorporated into the blend composition. Interfacially compatibilized TPE/nanodiamond composites, showed significant improved surface tribology and increased indentation and scratch resistance. Incorporation of nanodiamond particles into this TPE matrix, led to significant increase in thermal decomposition temperature (T_d).

References

1. Dahl, J. E. P.; Moldowan, J. M.; Peters, K. E.; Claypool, G. E.; Rooney, M. A.; Michale, G. E.; Mello, M. R.; Kohnen, M. L. Nature 1999, 399, 54.
2. Dahl, J. E.; Liu, S. G.; Carlson, R. M. K. Science 2003, 299, 96.
3. Carlson, R. M. K.; Dahl, J. E. P.; Liu, S. G.; Olmstead, M. M.; Buerki, P. R.; Gat, R. In Synthesis, Properties and Applications of Ultrananocrystalline Diamond; Gruen, D. M.; Shenderova, O. A.; Vul, A. Y., Eds.; Springer: New York, 2005; p 63.
4. Hala, S.; Landa, S. Angew Chem Int Ed 1966, 5, 1045.
5. Piekarczyk, W. Cryst Res Technol 1999, 24, 533.
6. Ristein, J. In Properties, Growth and Applications of Diamond; Nazare, M. H.; Neves, A. J., Eds.; Inspec: London, 2001; p 73.
7. Angus, J. C.; Hayman, C. C. Science 1988, 241, 913.
8. McKervey, M. A. Tetrahedron 1980, 36, 971.
9. Kristopher, D. B.; Antonella, S.; Vadym, M.; Guzeliya, K.; Gleb, Y.; Yury, G. ACS Nano 2009, 3, 363.
10. Shenderova, O.; Tyler, T.; Cunningham, G.; Ray, M.; Walsh, J.; Casulli, M.; Hens, S.; McGuire, G.; Kuznetsov, V.; Lipa, S. Diamond Related Mater 2007, 16, 1213.
11. Tyler, T.; Shenderova, O.; Cunningham, G.; Walsh, J.; Drobnik, J.; McGuire, G. Diamond Related Mater 2006, 15, 2078.
12. Dolmatov, V. Y. J Superhard Mater 2007, 29, 1.
13. Zheng, J.; Ozisik, R.; Siegel, R. W. Polymer 2005, 46, 10873.
14. Ghosh, A.; Sciamanna, S. F.; Dahl, J. E.; Liu, S.; Carlson, R. M. K. J Polym Sci 2007, 45, 1077.
15. Naimi-Jamal, M. R.; Kaupp, G. Macromol Symp 2008, 274, 72.
16. Zou, Q.; Wang, M.; Bin, L. V.; Yanguo, L. I.; Hui, Y. U.; Lianghua, Z.; Yucheng, Z. J Wuhan University Technol-Mater Sci Ed 2009, 24, 935.
17. Zou, Q.; Li, Y. G.; Lv, B.; Wang, M. Z.; Zou, L. H.; Zhao, Y. C. Inorganic Mater 2010, 46, 127.
18. Ito, T. Acta Crystallogr Sect B: Struct Crystallogr Cryst Chem 1973, 29, 346.
19. Evansa, E. H. M.; Hinea, R.; Richardsa, J. P. G. Solid State Commun 1978, 27, 1007.
20. VanLandingham, M. R.; Villarrubia, J. S. Macromol Symp 2001, 167, 15.